J. Membrane Biol. 192, 89–100 (2003)
DOI: 10.1007/s00232-002-1066-9

The Journal of
Membrane
Biology

Kinetic Mechanism of Na^+-Glucose Cotransport through the Rabbit Intestinal SGLT1 Protein

A. Berteloot
Groupe de Recherche en Transport Membranaire, Département de Physiologie, Faculté de Médecine, Université de Montréal, CP 6128, Succursale Centre-Ville, Montréal, QC H3C 3J7, Canada

Received: 9 July 2002/Revised: 19 November 2002

Abstract. No consensus has yet been reached regarding the order of substrate addition to the high-affinity Na^+-D-glucose cotransporter (SGLT1). This problem was addressed by computer-assisted derivation of the steady-state velocity equations characterizing the eight-state Na^+:Na^+:substrate (*NNS*) and Na^+:substrate:Na^+ (*NSN*) mechanisms of cotransport. A notable difference was found in their denominator expressions and used to device a new strategy aimed at model discrimination in which the initial rate data are recorded at fixed *S* and analyzed relative to the *N* dependence of transport using a Hill equation. According to this protocol, the values of the Hill coefficient (n_H) should be finite at all *S* ($1.0 < n_H \leqslant 2.0$) or decrease down to a limit value of 1.0 at high *S* in the case of the *NNS* and *NSN* models, respectively. These key experiments were performed in rabbit intestinal brush border membrane vesicles and demonstrated that a Hill equation with $n_H = 2.0$ best describes the steady-state kinetics of Na^+-glucose cotransport at all *S*. We therefore propose a kinetic mechanism whereby Na^+ binding should occur with very strong cooperativity within a rapid equilibrium segment of the transport cycle and be followed by a slow isomerization step before glucose addition.

Key words: Steady-state kinetics — Cotransport models — Substrate addition order — Discriminatory criteria — Rapid filtration technique — Brush-border membrane vesicles (rabbit jejunum)

Introduction

Secondary active transport is a fundamental biological principle [11, 32] best illustrated, over the last 40 years or so, by the high-affinity, Na^+-D-glucose cotransport system (SGLT1) [11, 17, 34, 39, 40]. The structural basis underlying the specific and efficient coupling of organic substrates (*S*) and Na^+ (*N*) fluxes is presently unknown. However, from a kinetic point of view, this mechanism is made possible through the formation of an intermediary complex involving *N*, *S*, and a membrane transport protein (*T*) [11, 32], hence the relevance of the question of substrate addition order to cotransport modeling. As regards SGLT1, available evidence indicates essential activation by *N* and 2*N*:1*S* coupling stoichiometry of cotransport [8, 18, 24, 39]. Accordingly, the so-called *NSN* and *NNS* models represent the only two sequential iso-ordered ter-ter mechanisms that prove compatible with these kinetic characteristics. Still, no consensus has yet been reached in the literature regarding which of these two models best describes the kinetics of glucose transport through the SGLT1 system [9, 17, 39], in part due to the lack of reliable kinetic criteria against which they can be discriminated.

A major obstacle in this respect appears to be the forbiddingly tedious algebraic manipulations involved in the derivation of initial velocity equations when steady-state assumptions are applied to 8-state mechanisms of cotransport [13]. Previous theoretical studies were thus performed using the simplifications introduced by the rapid equilibrium assumption (slow transfer across the membrane relative to membrane surface binding steps) [30] or the reduction to a 6-state model (the binding of the two *N* ions is described as a single reaction step) [28]. In both cases, the link be-

Abbreviations BBMV, brush-border membrane vesicles; BCA, bicinchoninic acid; FSRFA, fast-sampling, rapid-filtration apparatus; HEPES, N-[2-hydroxyethyl]-piperazine-N′-[2-ethanesulfonic] acid; *N*, Na^+ ion; *S*, substrate molecule (with indices i or o referring to internal or external *N* and *S*); SER, standard error of regression; SGLT1, high-affinity Na^+-D-glucose cotransporter; Tris, tris-[hydroxymethyl]-aminomethane.

Correspondence to: email: Alfred.Berteloot@umontreal.ca

tween the approximate and complete solutions is unknown and, in the second case, the *NNS* model is the only one to lend itself to simplification. Moreover, it was readily recognized in the original paper published by Restrepo and Kimmich [30] that their conclusion to an *NSN* model is valid only if the rapid equilibrium assumption holds. Similarly, it was recently shown by Falk et al. [13] that the reduction of an 8-state *NNS* mechanism to a 6-state model requires a number of explicit assumptions that were not given prominence in the original report of Parent et al. [28].

A different approach was used by Chen et al. [9] on the rationale that the leak pathways (phlorizin-sensitive *N* or H transport in the absence of external sugar) observed in *Xenopus* oocytes overexpressing the SGLT1 protein should demonstrate sigmoid or hyperbolic kinetics relative to ion concentrations if conforming to the *NNS* or *NSN* mechanisms, respectively. At the experimental level, it was shown that the *N*-leak involves a single ion; however, the H-leak appeared sigmoid rather than hyperbolic [9]. In addition, similar studies by Quick et al. [29] support the view that the Hill coefficient for *N* and H uniport is >1.2. Such discrepancies might be related to the difficulty to get reliable baseline values using phlorizin to inhibit ion transport through the SGLT1 protein because specific phlorizin binding to the transporter does not occur in *N*-free media or at more basic pH values [26]. In any event, as sound as it might be at the theoretical level, the *N* and/or H dependence of the leak pathway proved to be of low value as a kinetic criterion aimed at discriminating between the *NNS* and *NSN* mechanisms of cotransport.

Clearly, then, further progress in our search for a solution to the critical issue of which of the *NNS* or *NSN* models best accounts for transport kinetics through SGLT1 requires additional studies at the theoretical level. A first step in this direction was taken in the present studies through computer-assisted derivation of the zero-trans velocity equations characterizing the 8-state *NNS* and *NSN* mechanisms of cotransport. A notable difference was found in their denominator expressions and used to devise new kinetic criteria against which the two models can be discriminated. These key experiments were performed in rabbit intestinal brush border membrane vesicles (BBMV). It is concluded that the order of substrate addition is *N:N:S*, in which *N* binding should occur with very strong cooperativity within a rapid equilibrium segment of the transport cycle and be followed by a slow isomerization step before glucose addition.

Materials and Methods

Materials

Rabbits were purchased from the Maple Lane Farm (Clifford, Ontario). D-[1-^{3}H(N)]-glucose (specific activity 10–15 Ci/mmol) was supplied by New England Nuclear (NEN), the BCA (bicinchoninic acid) protein assay kit by Pierce, unlabeled D-glucose by Sigma, ultrapure salts by Aldrich, and amiloride hydrochloride and scintillation cocktail (Beta-Blend) by ICN Biomedicals. Cellulose nitrate filters (12.5 mM diameter, 0.65 μM pore size) were obtained from Micro Filtration Systems (MFS). All other chemicals were of the highest purity available.

Preparation of Rabbit Intestinal BBMV

BBMV were prepared from the jejunum of male, 2.0–2.5 kg New-Zealand white rabbits as described previously [10, 21]. Briefly, the P_2 fractions were frozen in liquid N_2, thawed on the day of use, and resuspended in 50 mM HEPES-Tris buffer (pH 7.0) containing 0.1 mM $MgSO_4$, 300 mM KI, 600 mM KCl, and 3 μM valinomycin to ensure full equilibration of the cation. BBMV were then prepared as a P_4 fraction and resuspended in the same buffer lacking the ionophore. To ensure stability of the preparations over the course of the experiments, 50 μL aliquots of BBMV were frozen in liquid N_2 until the time of assay. The protein concentration of these frozen vesicles was 28–35 mg/mL as estimated with the BCA assay kit using bovine serum albumin as a standard.

Transport Assays

Glucose transport was determined at 20°C under zero-trans gradient conditions using the fast-sampling, rapid-filtration apparatus (FSRFA) developed in our laboratory [4]. Briefly, for each assay, 40 μL of BBMV were thawed, prewarmed, and loaded into the apparatus. Uptake was initiated by injecting the vesicles into 460 μL of the incubation media. Final concentrations in the uptake assays were: 50 mM HEPES-Tris buffer (pH 7.0), 0.1 mM $MgSO_4$, 0.5 mM amiloride, 4 μM tracer D-glucose, and varying concentrations of unlabeled D-glucose (0, 0.02, 0.05, 0.1, 0.2, 0.5, and 1 mM) and N (0, 15, 30, 45, 60, 80, 100, 150, 200, 400, and 800 mM). Cation concentrations were kept constant at 900 mM by K^+ addition. The membrane potential was clamped to 0 mV by using a combination of iodide and chloride salts [3] to get total I^- and Cl^- concentrations of 300 and 600 mM, respectively. Three time course studies, consisting of a 9-point automatic sequential sampling of the uptake mixture (50 μL) at 1 s interval, were performed at each of these concentrations. Samples were injected into 1 mL of ice-cold stop solution, which consisted of 50 mM HEPES-Tris buffer (pH 7.0) containing 0.1 mM $MgSO_4$, 1 mM phlorizin, and 900 mM NaCl. The stopped mixture was filtered and washed three times with 1 mL of ice-cold stop solution. The substrate content of the vesicles was then determined by liquid scintillation counting as described previously [10, 21].

Data Analysis

The initial rates of glucose transport (v_i^S) were analyzed relative to outside *N* concentrations (N_o) using the modified Hill equation

$$v_i^S = v_i^0 + \frac{V_{max}^N (N_o)^{n_H}}{[(N_o)_{0.5}]^{n_H} + (N_o)^{n_H}} \quad (1)$$

in which v_i^0 represents the rate of tracer transport in the absence of *N* whereas V_{max}^N, $(N_o)_{0.5}$, and n_H stand, at each *S* concentration, for the apparent maximum rate of transport, *N* concentration yielding half-maximal velocity, and Hill coefficient, respectively. Nonlinear regression analyzes were performed using GraphPad Prism® (GraphPad Software, 1999, San Diego, CA), which can compare the fits of two equations using an *F* test. Note that the errors associated with the kinetic parameter values reported in this paper

represent the standard errors of regression (SER) on these parameters. Additional computations involved Mathematica in the derivation of Eqs. 6, 7, and 10.

Results

Model Derivations from Steady-State Assumptions

The 8-state sequential iso-ordered ter-ter mechanisms of Na^+-D-glucose cotransport analyzed in the present studies are depicted in Fig. 1. The two situations shown in *A* and *B* differ in the order of substrate binding to the transport protein, and these correspond to the *NNS* and *NSN* models with leak pathways as proposed by Parent et al. [28] and Chen et al. [9], respectively. Note that the assumption of mirror symmetry with regard to substrate binding introduced in these schemes does not affect in any way the generic form of velocity equations characterizing *S* transport under the zero-trans gradient conditions of both *N* and *S* used in the present studies. When derived from steady-state assumptions, v_i^S takes on the form

$$v_i^S = \frac{a_0 T_t (S_o)(N_o)^2}{b_0 + c_0(S_o) + [b_1 + c_1(S_o)](N_o) + [b_2 + c_2(S_o)](N_o)^2} \quad (2)$$

if meant to represent an experiment performed at fixed outside *S* (S_o) and varying N_o concentrations. In this equation, T_t stands for the total amount of transport protein, and the constant and substrate coefficient terms are macroconstants with algebraic expressions relative to the microscopic rate constants, as reported in Tables 1 and 2 for the *NNS* and *NSN* models, respectively. From these results, it clearly appears that Eq. 2 may apply to both models with the exception that the S_o substrate coefficient term c_0 should be set to zero in the denominator expression of the *NSN* mechanism as compared to its *NNS* counterpart.

New Kinetic Criteria Aimed at Model Discrimination

This notable difference in the velocity equations characterizing the *NNS* and *NSN* models of cotransport laid the foundations of new kinetic criteria against which they can be discriminated.

An important first observation is that Eq. 2 degenerates to

$$v_i^S = V_{max}^S = \frac{a_0 T_t (N_o)^2}{c_0 + c_1(N_o) + c_2(N_o)^2} \quad (3)$$

at high substrate concentrations, thus showing that the *N* dependence of transport under these experimental conditions should follow Hill-type kinetics in the case of the *NNS* mechanism but hyperbolic-type kinetics when $c_0 = 0$, as occurs for its *NSN* counterpart. The V_{max}^S notation used in Eq. 3 reflects the fact that its right-hand side expression would also represent the apparent V_{max} of transport in experiments where the initial rate data are recorded at fixed *N* concentrations and analyzed relative to the *S* dependence of transport. When studying the *N* dependence of transport, the validity of the test is constrained by the fact that it ought to be performed at close to saturating *S* concentrations. On the other hand, with regard to *v* over *S* plots, it might prove difficult to get reliable data at low *N* concentrations. Accordingly, as justified below, the analysis of the Hill coefficient over a whole range of *S* concentrations should constitute a more significant and robust test of the two models.

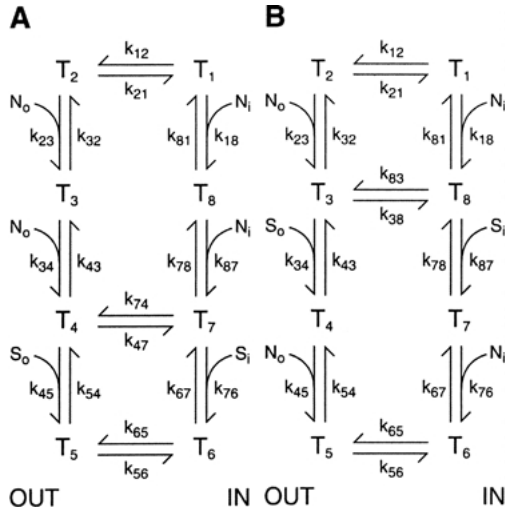

Fig. 1. Eight-state sequential iso-ordered ter-ter mechanisms of Na^+-D-glucose cotransport. The two situations shown in *A* and *B* differ in the order of substrate binding to the transport protein (*T*), and correspond to the *NNS* and *NSN* models with leak pathways (*N* transport in the absence of *S*) as proposed by Parent et al. [28] and Chen et al. [9], respectively. In both *A* and *B*, N_o and N_i stand for external (*OUT*) and internal (*IN*) Na^+, whereas S_o and S_i represent external and internal glucose, respectively.

Another important observation in this respect is that if the N_o coefficient term in the denominator expression of Eq. 2 is not small relative to the constant and N_o^2 coefficient terms at all *S*, then the velocity equation will not reduce to the Hill term appearing in Eq. 1. Nevertheless, velocity curves can always be expressed according to the Hill equation, in which case the Hill plot is a straight line only in the neighborhood of $v_i^S = V_{max}^N/2$ and the calculated n_H value is a fractional number < 2.0, the actual number of *N* binding sites [33]. Therefore, if the *N* dependence of transport is analyzed according to Eq. 1, the expected n_H value can be estimated from the quantity

Table 1. Derivation of the 8-state *NNS* mechanism of cotransport

Macro constants	Algebraic expressions
a_0	$k_{12}\,k_{23}\,k_{34}\,k_{45}\,k_{56}\,k_{67}\,k_{81}\,(k_{74}+k_{78})$
b_0	$k_{32}\,k_{81}\,(k_{12}+k_{21})\,(k_{54}\,k_{65}+k_{54}\,k_{67}+k_{56}\,k_{67})\,(k_{43}\,k_{74}+k_{43}\,k_{78}+k_{47}\,k_{78})$
b_1	$k_{81}\,(k_{54}\,k_{65}+k_{54}\,k_{67}+k_{56}\,k_{67})\,[k_{12}\,k_{23}\,(k_{43}\,k_{74}+k_{43}\,k_{78}+k_{47}\,k_{78})+k_{34}\,k_{47}\,k_{78}\,(k_{12}+k_{21})]$
b_2	$k_{23}\,k_{34}\,(k_{54}\,k_{65}+k_{54}\,k_{67}+k_{56}\,k_{67})\,[k_{12}\,k_{81}\,(k_{47}+k_{74}+k_{78})+k_{47}\,k_{78}\,(k_{12}+k_{81})]$
c_0	$k_{32}\,k_{45}\,k_{56}\,k_{67}\,k_{78}\,k_{81}\,(k_{12}+k_{21})$
c_1	$k_{45}\,k_{56}\,k_{67}\,k_{78}\,k_{81}\,(k_{12}\,k_{23}+k_{12}\,k_{34}+k_{21}\,k_{34})$
c_2	$k_{12}\,k_{23}\,k_{34}\,k_{45}\,k_{81}\,[k_{56}\,(k_{67}+k_{74}+k_{78})+(k_{65}+k_{67})\,(k_{74}+k_{78})]+k_{23}\,k_{34}\,k_{45}\,k_{56}\,k_{67}\,k_{78}\,(k_{12}+k_{81})$

The macro constants shown correspond to the constant and substrate coefficient terms appearing in Eq. 2 when applied to the *k*inetic mechanism of cotransport depicted in Fig. 1*A*.

$$n_H = \left[\frac{d\ln[v_i^S/(V_{max}^N - v_i^S)]}{d\ln(N_o)}\right]_{(N_o)_{0.5}} \tag{4}$$

where

$$V_{max}^N = \frac{a_0(S_o)T_t}{b_2 + c_2(S_o)} \tag{5}$$

represents the apparent maximum rate of transport observed at saturating N concentrations and

$$(N_o)_{0.5} = \frac{b_1 + c_1(S_o) + \sqrt{[b_1 + c_1(S_o)]^2 + 4[b_0 + c_0(S_o)][b_2 + c_2(S_o)]}}{2[b_2 + c_2(S_o)]} \tag{6}$$

is the calculated N_o concentration at which $v_i^S = V_{max}^N/2$. The formal development of Eq. 4 and subsequent rearrangements lead to

$$n_H = 1 + \frac{b_0 + c_0(S_o)}{b_0 + c_0(S_o) + [b_1 + c_1(S_o)](N_o)_{0.5}} \tag{7}$$

from which it can be concluded, in conjunction with the consideration of Eq. 6, that

$$n_H = 1 + \frac{b_0}{b_0 + b_1(N_o)_{0.5}} \quad \text{with} \quad (N_o)_{0.5} = \frac{b_1 + \sqrt{b_1^2 + 4b_0b_2}}{2b_2} \tag{8}$$

and that

$$n_H = 1 + \frac{c_0}{c_0 + c_1(N_o)_{0.5}} \quad \text{with} \quad (N_o)_{0.5} = \frac{c_1 + \sqrt{c_1^2 + 4c_0c_2}}{2c_2} \tag{9}$$

at low and high S concentrations, respectively.

Accordingly, the analysis of the n_H dependence on S concentrations provides us with a new kinetic criterion against which the *NNS* and *NSN* mechanisms of cotransport can be discriminated, as follows. In the case of the *NNS* mechanism (constant, and N_o and $N_o{}^2$ coefficient terms being present at all S), finite n_H values should be observed over the whole range of S concentrations ($1.0 < n_H \leqslant 2.0$ and correlation with S reflecting the relative values of the b_i and c_i coefficients). However, in the case of the *NSN* mechanism ($c_0 = 0$ and b_0 vanishing relative to the N_o and N_o^2 coefficient terms at increasing S concentrations), the n_H values should continuously decrease from a finite value recorded at low S down to the limit value of 1.0 at high S. The latter result was indeed expected from our analysis of Eq. 3, but the validity of the n_H dependence on S as a kinetic criterion aimed at model discrimination is not constrained by the question of whether a close to saturating S concentration is reached or not during the analysis. Yet, should there be any ambiguity in assessing whether the n_H value approaches 1.0 or not at high S, the following transformation of Eq. 7

$$\frac{1}{(N_o)_{0.5}}\left[\frac{1}{(n_H - 1)} - 1\right] = \frac{2 - n_H}{(N_o)_{0.5}(n_H - 1)} = \frac{b_1 + c_1(S_o)}{b_0 + c_0(S_o)} \tag{10}$$

could be used to analyze the S dependence of the new parameter appearing on the left-hand side, which can be calculated from the n_H and $(N_o)_{0.5}$ values estimated at each S concentration. Indeed, Eq. 10 predicts that either linear ($c_0 = 0$) or hyperbolic (upward when $c_1/c_0 > b_1/b_0$ but downward in the reverse case) behavior should be observed for the *NSN* or *NNS* mechanisms, respectively.

Table 2. Derivation of the 8-state *NSN* mechanism of cotransport

Macro constants	Algebraic expressions
a_0	$k_{12}\,k_{23}\,k_{34}\,k_{45}\,k_{56}\,k_{67}\,(k_{81} + k_{83})$
b_0	$k_{43}\,k_{78}\,(k_{12} + k_{21})\,(k_{54}\,k_{65} + k_{54}\,k_{67} + k_{56}\,k_{67})\,(k_{32}\,k_{81} + k_{38}\,k_{81} + k_{32}\,k_{83})$
b_1	$k_{23}\,k_{43}\,k_{78}\,(k_{54}\,k_{65} + k_{54}\,k_{67} + k_{56}\,k_{67})\,(k_{12}\,k_{38} + k_{12}\,k_{81} + k_{38}\,k_{81} + k_{12}\,k_{83}) + k_{45}\,k_{56}\,k_{67}\,k_{78}\,(k_{12} + k_{21})\,(k_{32}\,k_{81} + k_{38}\,k_{81} + k_{32}\,k_{83})$
b_2	$k_{23}\,k_{45}\,k_{56}\,k_{67}\,k_{78}\,(k_{12}\,k_{38} + k_{12}\,k_{81} + k_{38}\,k_{81} + k_{12}\,k_{83})$
c_0	0
c_1	$k_{12}\,k_{23}\,k_{34}\,k_{78}\,(k_{54}\,k_{65} + k_{54}\,k_{67} + k_{56}\,k_{67})\,(k_{81} + k_{83}) + k_{34}\,k_{45}\,k_{56}\,k_{67}\,k_{78}\,k_{81}\,(k_{21} + k_{21})$
c_2	$k_{12}\,k_{23}\,k_{34}\,k_{45}\,(k_{81} + k_{83})\,[k_{78}\,(k_{56} + k_{65} + k_{67}) + k_{56}\,k_{67}] + k_{23}\,k_{34}\,k_{45}\,k_{56}\,k_{67}\,k_{78}\,(k_{12} + k_{81})$

The macro constants shown correspond to the constant and substrate coefficient terms appearing in Eq. 2 when applied to the *k*inetic mechanism of cotransport depicted in Fig. 1*B*.

Discriminatory Value of the New Kinetic Criteria

The discriminatory value of the kinetic criteria established in the previous section needs to be evaluated with regard to potential modifications of Eq. 2, as may arise when involving simplifying assumptions such as equilibrium substrate binding. This was done through computer-assisted derivation of the velocity equations characterizing reduced *NNS* and *NSN* mechanisms of cotransport, which were generated by introducing one or more rapid equilibrium segments into the transport cycles depicted in Fig. 1. The results of these studies are summarized in Table 3, from which the following conclusions can be drawn.

First, full Eq. 2 only applies to *NNS* mechanisms and its generic form in this case is independent of whether *S* and/or the first *N* bind(s) to the protein in a steady-state or equilibrium reaction. In actual facts, then, full Eq. 2 characterizes steady-state *N* binding to the second of the two *N* sites.

Second, for *NSN* mechanisms, the simplification $c_0 = 0$ alone is independent of whether steady-state or rapid equilibrium assumptions are used to describe *N* binding to either one or both of the *N* sites and, then, appears to be a specific feature of steady-state *S* binding in this case. However, this same simplification also applies to *NNS* mechanisms if only the second of the two *N* ions binds within a rapid equilibrium segment, irrespectively of steady-state or equilibrium *S* binding. Accordingly, the kinetic criteria provided by Eqs. 3 and 7–10 should prove successful at assessing whether $c_0 = 0$ or not in Eq. 2: a negative answer in this respect would readily identify an *NNS* sequence of substrate addition to the transport protein, but a negative response ought to be interpreted with caution.

Third, the simplifications $c_0 = 0$ and $c_1 = 0$ in combination appear to be a specific feature of equilibrium *N* binding to both of the *N* sites in the case of *NNS* mechanisms, irrespectively of steady-state or equilibrium *S* binding. Clearly, this possibility should be easily identifiable from the demonstration that

Table 3. Modifications of Eq. 2 resulting from rapid equilibrium assumptions

Rapid equilibrium segments	Modifications of Eq. 2	
	NNS model	*NSN* model
T_2-T_3	None	$c_0 = 0$
T_3-T_4	$c_0 = 0$	$c_0 = b_2 = 0$
T_4-T_5	None	$c_0 = 0$
T_2-T_4	$c_0 = c_1 = 0$	$c_0 = b_2 = 0$
T_2-T_3 and T_4-T_5	None	$c_0 = 0$
T_3-T_5	$c_0 = 0$	$c_0 = b_2 = 0$
T_2-T_5	$c_0 = c_1 = 0$	$c_0 = b_2 = 0$

The rapid equilibrium segments shown were introduced into the kinetic mechanisms of cotransport depicted in Figs. 1*A* (*NNS* model) and 1*B* (*NSN* model). The effects of these modifications from the basic model were tested by computer-assisted derivation of the initial velocity equations characterizing each of the simplified schemes and subsequent comparison of their denominator expressions with that of Eq. 2 in the text.

V^S_{max} is independent of *N* concentrations, as inferred from Eq. 3. Note that Eq. 9 also indicates that, at saturating *S* concentrations, a Hill plot analysis of the data should prove meaningless in this case.

Last, the simplifications $c_0 = 0$ and $b_2 = 0$ in combination appear to be a specific feature of equilibrium *S* binding in the case of *NSN* mechanisms. This result is also independent of whether steady-state or rapid equilibrium assumptions are used to describe *N* binding to either one or both of the *N* sites. Clearly, the additional constraint $b_2 = 0$ does not affect in any way the predictive value of Eqs. 3–10 as regards discrimination against the *NNS* models (*see* second conclusion above). However, the concomitant demonstration that V^N_{max} is independent of *S* would readily identify a *NSN* sequence of substrate addition with rapid equilibrium *S* binding and rule out the concurrent *NNS* models, as inferred from Eq. 5.

Experimental Studies

In agreement with previous studies from our group [10, 25], the time courses of glucose transport re-

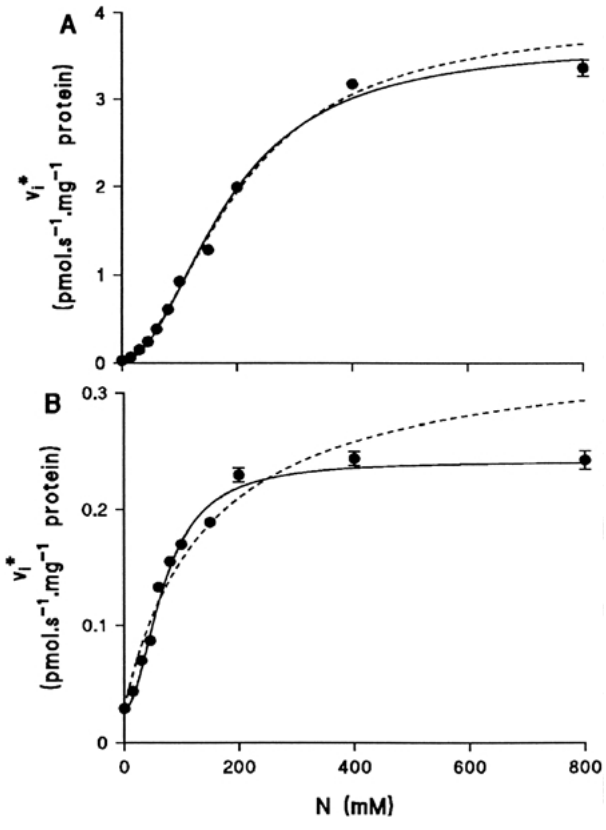

Fig. 2. *N* dependence of the initial rates of glucose transport v_i^* at low (*A*) and high (*B*) *S* concentrations. Uptake assays were performed as described in the text in the presence of 4 μM D-[1-^{3}H(N)]-glucose and either 0.020 (*A*) or 1.0 mM (*B*) unlabeled D-glucose. The best-fit lines to the data points (mean ± SD, $n = 3$) are shown, as determined by nonlinear regression analysis using Eq. 1 in the text. In *A*, n_H was used as a floating parameter (*dashed line*) or a prompt constant with integer value of 2.0 (*continuous line*). In *B*, n_H was used as a prompt constant with integer values of either 1.0 (*dashed line*) or 2.0 (*continuous line*). In both *A* and *B*, missing error bars were smaller than the symbol size.

corded in the present studies were found to be linear up to 7 s at all *S* and *N* concentrations (*results not shown*). Therefore, the initial rates of transport were estimated by linear regression analysis over the 1–7 s time course of the transport assays. For analytical purposes [5, 10, 22], glucose transport velocity measurements (v_i^*, pmol·s^{-1} · mg^{-1} protein) are expressed as tracer uptake rates at 4 μM radio-labeled glucose.

In the absence of *N*, tracer glucose transport proved to be independent of unlabeled *S* concentrations with finite intercept and slope values for the pooled data of 0.181 ± 0.011 pmol·mg^{-1} protein and 0.0292 ± 0.0024 pmol · s^{-1}·mg^{-1} protein, respectively. As illustrated in Fig. 2 at low (*A*) and high (*B*) glucose concentrations, the *N* dependence of transport was evaluated using Eq. 1 in which v_i^0 was fixed at the above slope value and n_H was first treated as a floating parameter (dashed line in Fig. 2*A*). The V_{max}^N dependence on *S* revealed by this analysis (Table 4) indicates that $b_2 \neq 0$ in Eq. 2, as inferred from Eq. 5. This result thus rules out all classes of *NSN* mechanisms with equilibrium *S* binding (Table 3). In addition, Table 4 clearly shows that the n_H data are randomly distributed above and below the mean value of 1.85 ± 0.23 over a range of *S* concentrations significantly affecting both V_{max}^N and $(N_o)_{0.5}$ (note also in this respect the 10-fold reduction in the *y* scales between Figs. 2*A* and *B*). As inferred from Eqs. 8 and 9, this result establishes that $c_o \neq 0$ in Eq. 2 and can be taken as evidence against all classes of *NSN* mechanisms.

In support of this view and validity of full Eq. 3, Fig. 2*B* (dashed line) and Table 4 demonstrate that the *N* dependence of transport observed at 1.004 mM glucose cannot be accounted for by hyperbolic kinetics when tested by treating n_H in Eq. 1 as a prompt constant with integer value of 1.0. In this respect, note that a run test shows significant deviation from model predictions when $n_H = 1.0$ ($p = 0.0397$). Moreover, the v_i^S dependence on *N* at close to saturating *S* also rules out all classes of *NNS* mechanisms with equilibrium *N* binding to both of the *N* sites for which $c_0 = c_1 = 0$ (Table 3).

The n_H data above support the concept that, within the experimental errors, the N_o coefficient term in the denominator expression of Eq. 2 is small relative to the constant and N_o^2 coefficient terms at all *S*. This assumption was further tested using Eq. 1 in which n_H was treated as a prompt constant with integer value of 2.0 (solid lines in Fig. 2*A* and *B*). The complete analysis is summarized in Table 4 from which we conclude, by looking at the *F* test, that the reduction in the degrees of freedom (number of data points minus number of variables) does not lead to a statistically significant decrease in the sum-of-squares at all glucose concentrations.

The finding that the observed n_H values are not significantly different from the actual number of *N* binding sites suggests that Eq. 1 fully accounts for the *N* dependence of transport at all *S*. As inferred from Eqs. 8–10, a n_H value of 2.0 at both low and high *S* would require that $b_1 = c_1 = 0$. Introducing these modifications into Eq. 2 and rearranging according to Cleland's nomenclature [33] thus lead to

$$v_i^S = \frac{V_{max}(S_o)(N_o)^2}{K_{mN}^2[K_{is} + (S_o)] + [K_{mS} + (S_o)](N_o)^2} \qquad (11)$$

with the following definitions of the new kinetic parameters: $V_{max} = a_0 T_t / c_2$, $K_{mS} = b_2/c_2$, $K_{mN}^2 = c_0/c_2$, and $K_{is} = b_0/c_0$. Note that the kinetic parameter $K_{in}^2 = b_0/b_2$ also needs to be defined for homogeneity of Eq. 11 with regard to the *S* dependence of transport, but that this parameter satisfies Eq. 12.

Table 4. *N* dependence of glucose transport

S (mM)	V^N_{max} (pmol·s^{-1}·mg^{-1} protein)	$(N_o)_{0.5}$ (mM)	n_H	*p* value of *F*-test
0.024	3.62 ± 0.10	185 ± 8	2.0 fixed	
	3.60 ± 0.14	183 ± 12	2.06 ± 0.1 8	0.745
0.054	2.94 ± 0.43	161 ± 18	2.0 fixed	
	3.50 ± 0.63	217 ± 50	1.68 ± 0.16	0.113
0.104	1.64 ± 0.13	132 ± 9	2.0 fixed	
	1.78 ± 0.18	147 ± 17	1.82 ± 0.12	0.213
0.204	1.05 ± 0.13	115 ± 12	2.0 fixed	
	1.31 ± 0.23	154 ± 33	1.62 ± 0.17	0.0902
0.504	0.577 ± 0.028	74 ± 7	2.0 fixed	
	0.569 ± 0.034	73 ± 8	2.20 ± 0.45	0.628
1.004	0.219 ± 0.010	69 ± 4	2.0 fixed	
	0.234 ± 0.013	79 ± 7	1.71 ± 0.13	0.095
	0.329 ± 0.054	183 ± 50	1.0 fixed	not necessary

The experiments depicted in Fig. 2 were repeated at me indicated glucose concentrations (*S*) to determine the apparent V^N_{max} and $(N_o)_{0.5}$ of transport. The *F*-test quantifies the relationship between the relative decrease in sum of squares and the relative decrease in degrees of freedom when going from the simpler (n_H value fixed at 2.0) to the more complex (floating n_H value) model. A *p* value > 0.05 indicates that there is no compelling evidence supporting the more complex model. At 1.004 mM glucose, the *F*-test proved to be not necessary (and, in real facts, just cannot be performed) when comparing Michaelis-Menten ($n_H = 1.0$) and Hill ($n_H = 2.0$) kinetics because the two models have identical degrees of freedom. Yet, the sum of squares and the relative errors associated with the V^N_{max} and $(N_o)_{0.5}$ values increased by a 3- to 5-fold factor when decreasing the n_H value to 1.0, thus showing that $n_H = 2.0$ significantly improves the goodness of fit. Moreover, comparing Hill kinetics with floating n_H values and Michaelis-Menten kinetics led to a *p* value < 0.0001, a highly significant figure as regards the goodness of the fit with the former model.

$$K^2_{in}K_{mS} = K_{is}K^2_{mN} \tag{12}$$

Comparing Eqs. 1 and 11 thus allows us to establish that

$$V^N_{max} = \frac{V_{max}(S_o)}{K_{mS} + (S_o)} \tag{13}$$

and

$$(N_o)^2_{0.5} = \frac{K^2_{mN}[K_{is} + (S_o)]}{K_{mS} + (S_o)} = \frac{K^2_{in}K_{mS} + K^2_{mN}(S_o)}{K_{mS} + (S_o)} \tag{14}$$

should represent valid analytical equations of the V^N_{max} and $(N_o)_{0.5}$ data for any candidate *NNS* kinetic mechanism that would conform to Eq. 11. Note that the right-hand term in Eq. 14 was obtained using Eq. 12 and proper substitution thereafter.

As shown in Fig. 3*A*, the V^N_{max} data reported in Table 4 satisfy the predictions of Eq. 13 when analyzed as a displacement curve of tracer glucose by unlabeled substrate as previously justified by our group [5, 10, 22]. It is thus possible to establish from these results that $V_{max} = 64 \pm 6$ pmol·s^{-1}·mg^{-1} protein and $K_{mS} = 43 \pm 8$ μM. Similarly, Fig. 3*B* demonstrates that the apparent $(N_o)_{0.5}$ data reported in Table 4 satisfy the predictions of Eq. 14 when using nonlinear regression analysis with the K_{mS} parameter fixed at the above value. It is thus possible to establish from these results that $K_{mN} = 50 \pm 4$ mM, $K_{in} = 230 \pm 6$ mM, and $K_{is} = 0.88 \pm 0.15$ mM.

Discussion

Theoretical Considerations

The theoretical studies presented in this paper demonstrate for the first time that, when derived from steady-state assumptions, the zero-trans velocity equations characterizing the 8-state *NNS* and *NSN* mechanisms of cotransport have similar generic forms, except for the absence of the substrate coefficient term c_o in the denominator expression of Eq. 2 characterizing the *NSN* model (Tables 1 and 2). This notable difference laid the foundations of a new strategy aimed at discriminating between the two models, which involves experiments where the initial rate data are recorded at fixed *S* and analyzed relative to the *N* dependence of transport using a Hill equation. If conforming to the *NNS* or *NSN* mechanisms, these data should show either finite values of the Hill coefficient at all *S* or decreasing values of this parameter down to a limit value of 1.0 at high *S*, respectively. Only two deviations from this general rule were noted with the *NNS* model and relate to the assumption that *N* binding to both sites or to the second site only is in rapid equilibrium (Table 3). The first eventuality can be readily identified from its associated characteristic Eq. 3 predicting the independence of V^S_{max} on *N* concentrations when $c_0 = c_1 = 0$. However, the second possibility also leads to $c_0 = 0$ in the denominator expression of Eq. 2 and, then, represents the unique limit case whereby the proposed approach will fail discrimination between the *N*:*N*:*S* and *N*:*S*:*N* sequences of substrate addition.

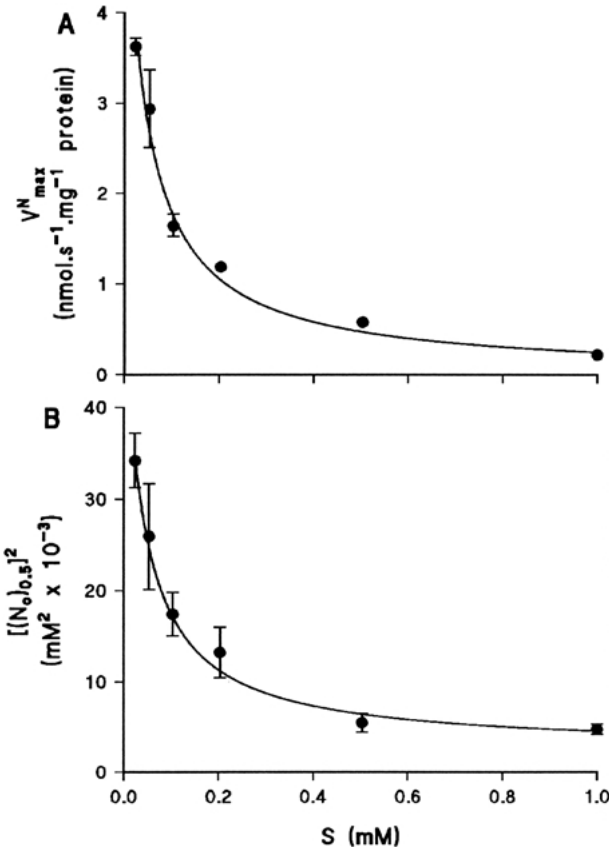

Fig. 3. *S* dependence of the V^{N}_{max} (*A*) and $(N_o)_{0.5}$ (*B*) data reported in Table 2 (n_H = 2.0). The best-fit lines are shown, as determined by nonlinear regression analysis using either Eq. 13 (*A*) or Eq. 14 (*B*) in the text. In both *A* and *B*, missing error bars were smaller than the symbol size.

Ordered *N:N:S* Sequence of Substrate Addition to the SGLTL Protein

When performed in rabbit intestinal BBMV, the key experiments discussed in the previous section proved to be a very useful and potent strategy to discriminate between representative members of the *NNS* and *NSN* mechanisms of Na^+-glucose cotransport. In this respect, these studies demonstrate that a Hill equation with n_H = 2.0 best describes the steady-state kinetics of glucose transport at all *S* (Fig. 2 and Table 4). Therefore, it can be unambiguously concluded that the two *N* ions bind first to the rabbit SGLT1 protein and that Eq. 11 fully accounts for the *S* dependence of both V^{N}_{max} and $(N_o)_{0.5}$ (Fig. 3). Moreover, the rearrangement of this equation according to Cleland's formalism [33] allowed us to estimate the four steady-state kinetic parameters relevant to Na^+-glucose cotransport under zero-trans gradient conditions.

A different conclusion with regard to the order of substrate binding was previously reached by Restrepo and Kimmich [30] on the observation that the V^{S}_{max} of α-methylglucose transport increases with *N* concentrations in chick intestinal epithelial cells. Indeed, within the context of rapid equilibrium kinetics advocated by these authors, it is readily apparent from Table 3 that the *NNS* model leads to a degenerate Eq. 2 involving the simplification $c_0 = c_1 = 0$ in its denominator expression. According to Eq. 3, then, the V^{S}_{max} dependence on *N* may appear as a valid kinetic criterion against which the *NNS* model should be rejected. However, as shown in Table 3 and in part correctly evaluated by Restrepo and Kimmich [30], the validity of this conclusion is highly restricted to equilibrium *N* binding to both of the *N* sites in the *NNS* mechanism. In addition, to be really conclusive with regard to the acceptability of the rapid equilibrium *NSN* model for which the simplification $c_0 = b_2 = 0$ ought to be introduced into the denominator expression of Eq. 2 (Table 3), the V^{S}_{max} dependence on *N* predicted from Eq. 3 should conform to hyperbolic kinetics. Notwithstanding the fact that such behavior is also expected if only the second of the two *N* ions binds within a rapid equilibrium segment of the *NNS* mechanism (Table 3), it turns out that the V^{S}_{max} dependence on *N* reported by Restrepo and Kimmich [30] appears to be sigmoid rather than hyperbolic at the close to saturating *S* concentration of 15 mM (n_H = 1.48 ± 0.22). Accordingly, this result and the concomitant consideration of Eqs. 6–9 strongly argue against, rather than support, the *NSN* mechanism of cotransport. In actual facts, as inferred from Eq. 5, the V^{S}_{max} dependence on *S* also reported by these authors [30] clearly rules out the rapid equilibrium *N*:*S*:*N* sequence of substrate addition.

Our conclusion of a *N*:*N*:*S* order of substrate binding to the SGLT1 protein agrees with that of Parent et al. [28] who further proposed a 6-state mechanism of cotransport whereby the addition of the two *N* ions on the transporter is described as a single reaction step. However, contrasting with our results at high *S* concentrations (Fig. 2*B*) and those of Restrepo and Kimmich [30] discussed above, the V^{S}_{max} of sugar transport was reported to be independent of *N* concentrations when estimated in *Xenopus* oocytes overexpressing the rabbit SGLT1 protein [27]. Quick et al. [29] recently argued that this result goes against the conclusion that *N* is the last substrate bound to the transporter. This conclusion is indeed supported by our theoretical studies and Eq. 3 when assuming equilibrium *N* binding to both of the *N* sites (in which case $c_0 = c_1 = 0$, *see* Table 3). However, this hypothesis proves to be internally inconsistent with other pieces of evidence reported by Parent et al. [27]. First, it cannot be accounted for by the velocity equation derived from the 6-state *NNS* model advocated by these authors, the generic form of which is fully compatible with that proposed for Eq. 11 in the present studies [13, 28]. Second, it would conflict with the predictions of Eqs. 8 and 9 as regards the obser-

vation of n_H values ≈2.0 at all S from 0.1 to 20 mM and the finding of finite $(N_o)_{0.5}$ values at high S concentrations [27]. Last, it would prove incompatible with the concomitant demonstration of the V^S_{max} dependence on membrane potential because more negative potentials, which decrease the apparent $(N_o)_{0.5}$ of transport [27], merely act by increasing the effective N concentration acting on the SGLT1 protein. Therefore, the N independence of V^S_{max} reported by Parent et al. [27] can be seriously questioned as regards the lowest N concentration used in their studies (10 mM) and/or the stability over time of the oocyte preparation when varying N concentrations from 10 to 100 mM in this order.

Kinetic Mechanism of Na^+-Glucose Cotransport through the SGLT1 Protein

The demonstration that Eq. 11 fully accounts for the steady-state kinetics of Na^+-glucose cotransport does not tell us which modifications should be introduced into the general 8-state mechanism depicted in Fig. 1*A* to justify the absence of the substrate coefficient terms b_1 and c_1 in the denominator expression of Eq. 2. As a starting point to resolve this issue, it should be noted that the 6-state model of Parent et al. [28] satisfies these requirements. However, the two empirical assumptions seemingly supporting this reduction of the 8-state mechanism (either the binding of the first N is much faster than the second or the two N bind with identical rate constants to similar sites [28]) have since been dismissed following their critical evaluation by Falk et al. [13]. As further shown in the latter studies, the only way to justify the fusion of two discrete N binding steps into a single reaction sequence (and, hence, that $b_1 \approx 0$) is to assume that the addition of the two N ions is random and occurs with very strong cooperativity within a rapid equilibrium segment of the transport cycle. Interestingly, this predicted high degree of cooperativity between the two N sites has since been demonstrated [23]. Yet, as clearly apparent from Table 3, this assumption alone would also introduce the additional constraints that $c_0 = 0$ and $c_1 = 0$, the combination of which proves to be incompatible with the experimental data reported in this and previous studies [27, 30] (*see* Discussion above). This seemingly paradoxical issue was resolved by Falk et al. [13] on the additional hypothesis of the existence of a slow isomerization step consecutive to N binding but preceding S addition to the SGLT1 protein, in which case $c_1 = 0$ but $c_0 \neq 0$. Moreover, as far as the generic form of Eq. 11 is concerned, it does not matter whether S binding is in rapid equilibrium or not and whether the Na^+-leak pathway occurs upstream or downstream from the slow isomerization step [13]. Therefore, the kinetic scheme depicted in Fig. 4*A*

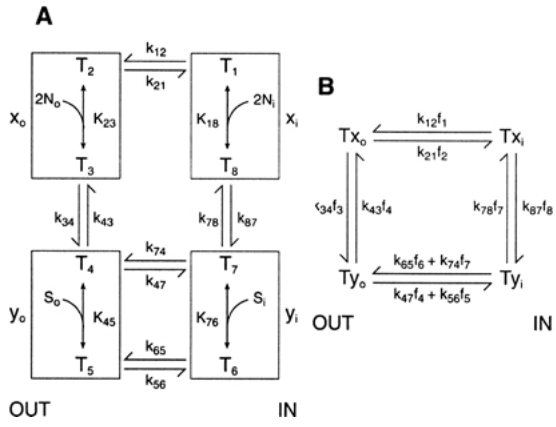

Fig. 4. Proposed 8-state mechanism of Na^+-D-glucose cotransport. (*A*) It is assumed that the addition of the two Na^+ ions (N) is random and occurs with very strong cooperativity within a rapid equilibrium segment of the transport cycle, hence justifying the fusion of two discrete N binding steps into a single reaction sequence [13]. The 2 N-bound complex (T_3) is committed to a slow isomerization step leading to "deocclusion" of the S binding site. The reorientation of this site from an outward- to an inward-facing configuration can proceed in the complete absence of S (T_4/T_7 transition, leak pathway) or following rapid equilibrium binding of S (T_5/T_6 transition, cotransport pathway). Note that the latter assumption does not affect the generic form of Eq. 11 [13]. (*B*) Equivalent 4-state scheme of the model depicted in *A* after reduction according to Cha's formalism [7] in which the T_X and T_Y species represent the summation of those carrier species linked through a rapid equilibrium segment, whereas the f_i stand for the fractional concentrations of the different T_i species. Other notations are as described in the legend to Fig. 1. Under zero-trans conditions, note that $f_1 = f_7 = 1$ and $f_6 = f_8 = 0$, whereas $f_2 = K_{23}/[K_{23} + (N_o)^2]$, $f_3 = (N_o)^2/[K_{23} + (N_o)^2]$, $f_4 = K_{45}/[K_{45} + (S_o)]$, and $f_5 = (S_o)/[K_{45} + (S_o)]$.

represents the simplest 8-state mechanism of cotransport that can be used as a fully justified substitute for the empirical 6-state model of Parent et al. [28]. Indeed, as shown in Table 5, this kinetic mechanism does fulfill the requirements of Eq. 11 and would readily account for the ligand-induced conformational changes recently inferred from fluorescence studies of human SGLT1 [23]. Note in Fig. 4*A* that the positioning of the leak pathway at the T_4/T_7 rather than T_3/T_8 transition is compatible with the concept that the 2-N-bound complex (T_3) is committed to a slow isomerization step leading to "deocclusioin" of the S binding site. Accordingly, the reorientation of this site from an outward- to an inward-facing configuration could proceed, although at a slower rate, in the complete absence of S.

It was recently argued [40] that the gain in simplifying an 8-state mechanism (20 rate constants) to a 6-state model (14 rate constants) outweighs the more rigorous approach proposed by Falk et al. [13]. We cannot subscribe to this simplistic view for at least two main reasons. First, as inferred from Fig. 4*A* and previously discussed [13], at least 4 out

Table 5. Derivation of the pseudo 8-state *NNS* mechanism of cotransport

Macro constants	Algebraic expressions
a_0	$k_{12}\ k_{34}\ k_{56}\ (k_{74} + k_{78})$
b_0	$(k_{12} + k_{21})\ (k_{43}\ k_{74} + k_{43}\ k_{78} + k_{47}\ k_{78})$ $K_{23}\ K_{45}$
b_1	0
b_2	$[k_{12}\ (k_{34} + k_{43})\ (k_{74} + k_{78}) + k_{47}$ $(k_{12}\ k_{34} + k_{37}\ k_{78} + k_{12}\ k_{78})]\ K_{45}$
c_0	$k_{56}\ k_{78}\ (k_{12} + k_{21})\ K_{23}$
c_1	0
c_2	$k_{12}\ k_{34}\ (k_{56} + k_{74} + k_{78}) + k_{56}\ k_{78}$ $(k_{12} + k_{34})$

The macro constants shown correspond to the constant and substrate coefficient terms appearing in Eq. 2 when applied to the kinetic mechanism of cotransport depicted in Fig. 4*A*.

of the 14 rate constants appearing in the 6-state model of Parent et al. [28] ought to be pseudo rate constants, the value of which may change with *N* concentrations and/or membrane potential. In support of this view, the k_{21}/k_{12} ratio of 24 previously reported by these authors [28] has since been reevaluated to the value of 1000 from parallel measurements of presteady-state currents and fluorescent changes [23]. Second, the 8-state mechanism depicted in Fig. 4*A* is characterized by 12 independent parameters out of its 10 rate constants and 4 dissociation constants (two of these are linked to the others through the law of microscopic reversibility applying to the two cycles). In this respect, then, this model is in no way more complex than its 6-state counterpart, which is also characterized by 12 independent parameters out of its 14 rate constants. In actual facts, its derivation is even simpler because it can be transformed to an equivalent 4-state scheme according to Cha's formalism [7] (Fig. 4*B*), so that 4 rather than 15 King-Altman patterns need to be considered. It is therefore our contention that the more rigorous analyses introduced in the present and previous studies [13] surpass in every respect the empirical treatment of the 6-state model [23, 28, 29].

Comparison of Sugar Transport and Phlorizin Binding Studies

The *N*:*N*:*S* sequence of *N* and glucose addition proposed in the present studies for the rabbit intestinal SGLT1 protein contrasts with the previously established *N*:*S*:*N* order of *N* and phlorizin binding to rabbit kidney BBMV [26]. It could be argued that these seemingly contradictory results are linked to the molecular heterogeneity of Na^+-glucose cotransport in the kidney as compared to the small intestine [40]. However, such an explanation appears unlikely because a similar paradigm also emerges from the sugar transport and phlorizin binding studies of Restrepo and Kimmick [30, 31]. As discussed in a previous section, α-methylglucose transport in chick intestinal cells [30] appears to be fully compatible with an *N*:*N*:*S* sequence of *N* and sugar addition when reevaluated in the light of our theoretical studies. Yet, phlorizin binding in similar cell preparations [31] rather conforms to an *N*:*S*:*N* order of *N* and inhibitor binding to the transport protein, as can be unambiguously concluded from the demonstration that phlorizin dissociation is much faster in the absence than in the presence of *N* [26, 31]. All together, these data thus seem to challenge the classical view that Na^+-glucose cotransport modeling can be probed using the binding kinetics of a nontransported competitive inhibitor like phlorizin [38].

In this regard, the cotransporter has receptor sites for both glucose and phloretin, the aglucone moiety of the phlorizin molecule [1]. Moreover, phlorizin inhibition of glucose transport is fast on the steady-state time scale of 0–9 s [25] whereas phlorizin binding to BBMV requires several minutes to reach equilibrium [2, 26, 31]. This so-called fast-acting slow-binding paradigm [14] has since been solved by showing that phlorizin binding is a two-step process whereby fast *N* and inhibitor addition to both of the sugar and aglucone sites is followed by a slow conformation change preceding further *N* attachment, thus occluding and stabilizing that part of the phlorizin-bound receptor complexes detected using a rapid filtration assay [26]. Accordingly, one may question the significance of a direct comparison between two molecules showing different binding properties to their receptor protein.

As an alternative and/or complementary consideration, it should further be noted that the theoretical studies reported in the present paper were constrained to the hypothesis that SGLT1 functions as a monomeric protein. While seemingly supported by freeze-fracture electron microscopic examination of recombinant cotransport protein expressed in oocytes [12, 41], this assumption may, however, conflict with inactivation radiation [35–37] as well as other studies [6, 10, 15, 16, 19, 20, 25, 26] performed in native intestinal and renal membranes. Accordingly, the *N*:*N*:*S* sequence of *N* and sugar addition vs the *N*:*S*:*N* order of *N* and phlorizin binding to the SGLT1 protein might as well represent two complementary aspects of a more complex mechanism that remains to be identified.

This research was supported by grant MT-14407 from the Canadian Institutes for Health Research (CIHR). The technical assistance of Mrs. C. Leroy has been greatly appreciated. The author also thanks C. Chenu and S. D. Patil for insightful discussions, and C. Gauthier for the art work.

References

1. Alvarado, F. 1 967. Hypothesis for the interaction of phlorizin and phloretin with membrane carriers for sugars. *Biochim. Biophys. Acta* **135:**483–495
2. Aronson, P. 1978. Energy-dependence of phlorizin binding to isolated renal microvillus membranes. *J. Membrane Biol.* **42:**81–98
3. Berteloot, A. 1986. Membrane potential dependency of glutamic acid transport in rabbit jejunal brush-border membrane vesicles: K^+ and H^+ effects. *Biochim. Biophys. Acta* **861:**447–456
4. Berteloot, A., Malo, C., Breton, S., Brunette, M. 1991. A fast sampling, rapid filtration apparatus: principal characteristics and validation from studies of D-glucose transport in human jejunal brush-border membrane vesicles. *J. Membrane Biol.* **122:**111–125
5. Berteloot, A., Semenza, G. 1990. Advantages and limitations of vesicles for the characterization and kinetic analysis of transport systems. *Meth. Enzymol.* **192:**409–437
6. Blank, ME., Bode, F., Baumann, K., Diedrich, D.F. 1989. Computer analysis reveals changes in renal Na^+-glucose cotransporter in diabetic rats. *Am. J. Physiol.* **257:**C385–C396
7. Cha, S. 1968. A simple method for derivation of rate equations for enzyme-catalyzed reactions under the rapid equilibrium assumption or combined assumptions of equilibrium and steady-state. *J. Biol. Chem.* **243:**820–825
8. Chen, X.-Z., Coady, M., Jackson, F., Berteloot, A., Lapointe, J.-Y. 1995. Thermodynamic determination of the Na^+-glucose coupling ratio for the human SGLT1 cotransporter. *Biophys. J.* **69:**2405–2414
9. Chen, X.-Z., Coady, M., Jalal, F., Wallendorf, B., Lapointe, J.-Y. 1997. Sodium leak pathway and substrate binding order in the Na^+-glucose cotransporter. *Biophys. J.* **73:**2503–2510
10. Chenu, C., Berteloot, A. 1993. Allosterism and Na^+-D-glucose cotransport kinetics in rabbit jejunal vesicles: compatibility with mixed positive and negative cooperativities in a homo-dimeric or tetrameric structure and experimental evidence for only one transport protein involved. *J. Membrane Biol.* **132:**95–113
11. Crane, R.K. 1977. The gradient hypothesis and other models of carrier-mediated active transport. *Rev. Physiol. Biochem. Pharmacol.* **78:**99–159
12. Eskandary, S., Wright, E.M., Kreman, M., Starace, D.M., Zampighi, G.A. 1998. Structural analysis of cloned plasma membrane proteins by freeze-fracture electron microscopy. *Proc. Natl. Acad. Sci. USA* **95:**11235–11240
13. Falk, S., Guay, A., Chenu, C., Patil, S.D., Berteloot, A. 1998. Reduction of an eight-state mechanism of cotransport to a six-state model using a new computer program. *Biophys. J.* **74:**816–830
14. Falk, S., Oulianova, N., Berteloot, A. 1999. Kinetic mechanisms of inhibitor binding: relevance to the fast-acting slow-binding paradigm. *Biophys. J.* **77:**173–188
15. Gerardi-Laffin, C., Delque-Bayer, P., Sudaka, P., Poirée, J.C. 1993. Oligomeric structure of the sodium-dependent phlorizin binding protein from kidney brush-border membranes. *Biochim. Biophys. Acta* **1151:**99–104
16. Giudicelli, J., Bertrand, M.-F., Bilski, S., Tran, T.T., Poirée, J.-C. 1998. Effect of cross-linkers on the structure and function of pig-renal sodium-glucose cotransporters after papain treatment. *Biochem. J.* **330:**733–736
17. Kimmich, G.A. 1990. Membrane potentials and the mechanism of intestinal Na^+-dependent sugar transport. *J. Membrane Biol.* **114:**1–27
18. Kimmich, G.A., Randles, J. 1980. Evidence for an intestinal Na^+-sugar transport coupling stoichiometry of 2,0. *Biochim. Biophys. Acta* **596:**439–444
19. Koepsell, H., Fritzsch, G., Korn, K., Madrala, A. 1990. Two substrate sites in the renal Na^+-D-glucose cotransporter studied by model analysis of phlorizin binding and D-glucose transport measurements. *J. Membrane Biol.* **114:**113–132
20. Koepsell, H., Spangenberg, J. 1994. Function and presumed molecular structure of Na^+-D-glucose cotransport systems. *J. Membrane Biol.* **138:**1–11
21. Maenz, D.D., Chenu, C., Bellemare, F., Berteloot, A. 1991. Improved stability of rabbit and rat intestinal brush border membrane vesicles using phospholipase inhibitors. *Biochim. Biophys. Acta* **1069:**250–258
22. Malo, C., Berteloot, A. 1991. Analysis of kinetic data in transport studies: new insights from kinetic studies of Na^+-D-glucose cotransport in human brush-border membrane vesicles using a fast sampling, rapid filtration apparatus. *J. Membrane Biol.* **122:**127–141
23. Meinild, A.K., Hirayama, B.A., Wright, E.M., Loo, D.D. 2002. Fluorescence studies of ligand-induced conformational changes of the Na^+/glucose cotransporter. *Biochemistry* **29:**1250–1258
24. Moran, A., Davis, L.J., Turner, R.J. 1988. High affinity phlorizin binding to the LLC-PK_1 cells exhibits a sodium phlorizin stoichiometry of 2:1. *J. Biol. Chem.* **263:**187–192
25. Oulianova, N., Berteloot, A. 1996. Sugar transport heterogeneity in the kidney: two independent transporters or different transport modes through an oligomeric protein? 1. glucose transport studies. *J. Membrane Biol.* **153:**181–194
26. Oulianova, N., Falk, S., Berteloot, A. 2001. Two-step mechanism of phlorizin binding to the SGLT1 protein in the kidney. *J. Membrane Biol.* **179:**223–242
27. Parent, L., Supplisson, S., Loo, D.D.F., Wright, E.M. 1992. Electrogenic properties of the cloned Na^+/glucose cotransporter. I. Voltage-clamp studies. *J. Membrane Biol.* **125:**49–62
28. Parent, L., Supplisson, S., Loo, D.D.F., Wright, E.M. 1992. Electrogenic properties of the cloned Na^+/glucose cotransporter: II. A transport model under nonrapid equilibrium conditions. *J. Membrane Biol.* **125:**63–79
29. Quick, M., Loo, D.D., Wright, E.M. 2001. Neutralization of a conserved amino acid residue in the human Na^+/glucose (hSGLTl) generates a glucose-gated H^+ channel. *J. Biol. Chem.* **19:**1728–1734
30. Restrepo, D., Kimmich, G.A. 1985. Kinetic analysis of mechanism of intestinal Na^+-dependent sugar transport. *Am. J. Physiol.* **248:**C498–C509
31. Restrepo, D., Kimmich, G.A. 1986. Phlorizin binding to isolated enterocytes: Membrane potential and sodium dependence. *J. Membrane Biol.* **89:**269–280
32. Schultz, S.G., Curran, P.F. 1970. Coupled transport of sodium and organic solutes. *Physiol. Rev.* **50:**637–718
33. Segel, I.H. 1975. Steady-state kinetics of multireactant enzymes. *In:* Enzyme kinetics: behavior and analysis of rapid equilibrium and steady-state enzyme systems. J. Wiley & Sons, editor. Wiley-Interscience, New York, pp. 505–845
34. Semenza, G., Kessler, M., Hosang, M., Weber, J., Schmidt, U. 1984. Biochemistry of the Na^+, D-glucose cotransporter of the small-intestinal brush-border membrane. The state of the art in 1984. *Biochim. Biophys. Acta* **779:**343–379
35. Stevens, B.R., Fernandez, A., Hirayama, B., Wright, E.M., Kempner, E.S. 1990. Intestinal brush border membrane Na^+/glucose cotransporter functions in situ as a homotetramer. *Proc. Natl. Acad. Sci. USA* **87:**1456–1460
36. Takahashi, M., Malathi, P., Preiser, H., Jung, C.Y. 1985. Radiation inactivation studies on the rabbit kidney sodium-

dependent glucose transporter. *J. Biol. Chem.* **260:**10551–10556

37. Turner, R.J., Kempner, E.S. 1982. Radiation inactivation studies of the renal brush-border membrane phlorizin-binding protein. *J. Biol. Chem.* **257:**10794–10797
38. Turner, R.J., Silverman, M. 1980. Testing carrier models of cotransport using the binding kinetics of non-transported competitive inhibitors. *Biochim. Biophys. Acta.* **596:**272–291
39. Wright, E.M. 1993. The intestinal Na^+/glucose cotransporter. *Annu. Rev. Physiol.* **55:**575–589
40. Wright, E.M. 2001. Renal Na^+/glucose cotransporters. *Am. J. Physiol.* **280:**F10–F18
41. Zampighi, G.A., Kreman, M., Boorer, K.J., Loo, D.D., Bezanilla, F., Chandy, G., Hall, J.E., Wright, E.M. 1995. A method for determining the unitary functional capacity of cloned channels and transporters expressed in *Xenopus laevis* oocytes. *J. Membrane Biol.* **148:**65–78